Square Wave Adsorptive Stripping Voltammetry of Nickel and Cobalt at Wall-Jet Electrodes in Continuous Flow

Christopher M.A. Brett,[*+] *M. Beatriz Quinaz Garcia,*[++] and *José L.F.C. Lima*[++]

[+] Departamento de Qumica, Universidade de Coimbra, P-3049 Coimbra, Portugal
[++] Departamento de Química-Física, Faculdade de Farmácia, Universidade do Porto, Rua Anibal Cunha, P-4000 Porto, Portugal

Received: January 11, 1996
Final version: April 22, 1996

Abstract
Square wave adsorptive stripping voltammetry (SWAdSV) of nickel and cobalt at wall-jet electrodes in a continuous flow system has been evaluated. Characteristics and advantages relative to differential pulse adsorptive stripping voltammetry (DPAdSV) in continuous flow systems are explored. Under optimized experimental conditions, sensitivity is approximately a factor of ten higher than DPAdSV, and one-nanomolar detection limits are achieved. Solution deoxygenation is unnecessary and sample throughput is increased.

Keywords: Adsorptive stripping voltammetry, Wall-jet electrode, Square wave voltammetry, Nickel, Cobalt, Trace metals

1. Introduction

Cobalt and nickel belong to the class of elements considered essential for man, animals and plants [1]. Cobalt is a component of Vitamin B12 and nickel is necessary for a number of metabolic processes. Variations in the small quantities necessary in the normal physiological state can cause toxicity or deficiency problems. There is thus a clear need for the determination of trace, i.e., ppb and sub-ppb, levels of these elements. Using electroanalytical procedures, the necessary preconcentration of the elements in the analyte can be performed in situ which is not possible with other analytical techniques such as atomic absorption spectroscopy. The development of continuous-flow electrochemical preconcentration methods has become an important area of research [2], and in combination with preconcentration makes on-line monitoring possible.

The electroanalysis of traces of cobalt and nickel ions can be carried out by anodic stripping voltammetry (ASV) or adsorptive stripping voltammetry (AdSV). ASV procedures are affected by slow kinetics in the reoxidation (determination) step. To overcome this problem a ligand such as thiocyanate is added to the solution to increase the rate of the electrooxidation reaction and detection limits of 5×10^{-8} M can then be attained [3]. Adsorptive stripping voltammetry [4] is superior from an analytical point of view, particularly regarding the attainment of lower detection limits. It involves the nonelectrolytic preconcentration by accumulation of the Ni^{II} and Co^{II} species-specific oxime complexes in the +2 oxidation state on the surface of a mercury electrode. In the determination step a negative potential scan leads to reduction to the zero oxidation state, the metal then dissolving in the mercury [5].

Initial studies were carried out at hanging mercury drop electrodes in ammonia buffer containing the dimethylglyoxime ligand using a differential pulse scan in the determination step (DPAdSV) [5,6]. More recent studies at this type of electrode have used other oxime ligands such as nioxime (1,2-cyclohexanedione dioxime) [7]; square wave voltammetry has also been investigated [8].

Instead of a hanging mercury drop electrode, a mercury thin-film electrode may be employed. Recently the determination of cobalt and nickel at a rotating disk mercury thin film electrode [9] and in continuous flow at a wall-jet mercury thin-film electrode [10] were demonstrated. In the wall-jet research [10], the optimum experimental conditions for DPAdSV used nioxime ligand in HEPES biological buffer with sodium perchlorate electrolyte as carrier solution. Preconcentration was done at −0.7 V (vs. Ag/AgCl, 0.1 M KCl) and the determination step involved reduction through a differential pulse negative-going scan to −1.3 V. In this way concentrations down to 1 nM (ca. 0.06 μg L^{-1}) could be measured.

The objective of this work was the development of a square wave (SW) AdSV procedure for wall-jet electrodes in continuous flow systems. General advantages of square wave voltammetry [11] are its rapidity and good discrimination against background currents and interfences, including dissolved oxygen [12]. Thus, after optimization of the experimental procedure and square wave parameters, the relative merits of square wave AdSV were examined with respect to differential pulse AdSV, particularly regarding the removal of oxygen, sample throughput, sensitivity and detection limit.

2. Experimental

All experiments were done using a computer-controlled PSTAT10 Autolab potentiostat (Eco-Chemie, Utrecht, Netherlands). A wall-jet cell (Oxford Electrodes) contained a glassy carbon working electrode of diameter 3.0 mm. The nozzle-electrode separation was maintained at 3.0 mm in all experiments and the nozzle diameter was 0.345 mm. A platinum tube counter electrode was placed in the cell exit and the Ag/AgCl (3.0 M KCl) reference electrode was in a separate compartment separated from the main body of the cell by a porous glass frit. The glassy carbon working electrode was polished prior to mercury film formation with diamond spray (Kemet International Ltd.) down to 1 μm particle size on a polishing cloth.

The continuous flow system consisted of a Gilson Miniplus 3-way peristaltic pump (flow rate regulated between 0.035 and 0.045 $cm^3 s^{-1}$), pulse dampers, and a two-way valve for switching between the solution employed for forming the mercury film on the glassy carbon substrate and the analyte solution.

All reagents were of analytical grade. Nioxime (1,2-cyclohexanedione dioxime) was obtained from Aldrich and HEPES (hemisodium salt of *N*-[2-hydroxyethyl]piperazine-*N*'-[2-ethanesulfonic acid]), pK_a 7.4, from Sigma Chemical Co. All solutions were made with Millipore Milli-Q ultrapure water, resistivity > 18 MΩ cm. Microliter volumes of stock solutions of Co and Ni (10^{-3} M) were added to electrolyte solution using

  1040-0397/96/1212-1169 $ 10.00+.25/0

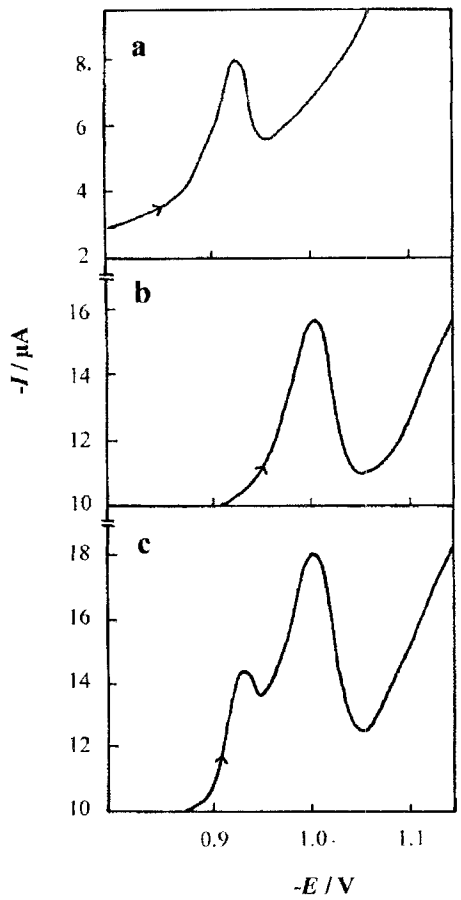

Fig. 1. Typical square wave AdSV results at wall-jet mercury thin-film electrode in 30 mM HEPES/0.1 M $NaClO_4$ electrolyte for a) Ni^{2+} (1.00×10^{-8} mol dm^{-3}); b) Co^{2+} (1.00×10^{-8} mol dm^{-3}); c) Ni^{2+} and Co^{2+} (both 1.00×10^{-8} mol dm^{-3}). Flow rate, $V_f = 0.035$ cm^3 s^{-1}. Conditions: $f = 40$ Hz; $h = 30$ mV and $t_{ads} = 60$ s.

Gilson micropipettes immediately before analysis and after appropriate dilution. The supporting electrolyte was 30 mM HEPES in 0.1 M sodium perchlorate. All experiments were conducted at room temperature (22–23 °C).

The mercury thin film was formed prior to determination of cobalt or nickel by electrodeposition at −1.0 V (vs. Ag/AgCl) for 300 s under continuous flow conditions from a solution containing 10^{-4} M Hg^{2+} either in 0.1 M KNO_3 + 5 mM HNO_3 or in 30 mM HEPES + 0.1 M $NaClO_4$ supporting electrolyte. Equally good, reproducible results were obtained from mercury films formed in both media.

3. Results and Discussion

Typical square wave voltammograms for the adsorptive stripping voltammetry of nickel and cobalt are shown in Figure 1. Adsorption on the mercury thin film electrode surface was carried out at −0.7 V (vs. Ag/AgCl) [8] and the square wave scan done in a negative direction from −0.7 V to −1.2 V in order to reduce the adsorbed metal ion-nioxime complex to the metal. It can be seen that the cobalt signal is larger than that of nickel. This will be further discussed below.

Peak potentials in Figure 1 are −0.925 V for nickel and −1.005 V for cobalt, under the experimental conditions specified, independent of whether the two ions are analyzed separately or in a mixture. The values obtained differ from those found previously with DPAdSV at the wall-jet electrode [8] (−0.94 V and −1.01 V, respectively) for two reasons: mainly because the peak potential varies with square wave frequency and with square wave amplitude and secondly because a different concentration of potassium chloride was used in the reference electrode compartment (3 M vs. 0.1 M).

The asymmetric form of the peaks obtained in the determination step is evident in Figure 1. In anodic stripping voltammetry with convective flow this is due to hydrodynamic effects, since the metal ion product of the electrode reaction in the determination step is swept away from the region close to the surface of the wall-jet electrode into the bulk solution [13].

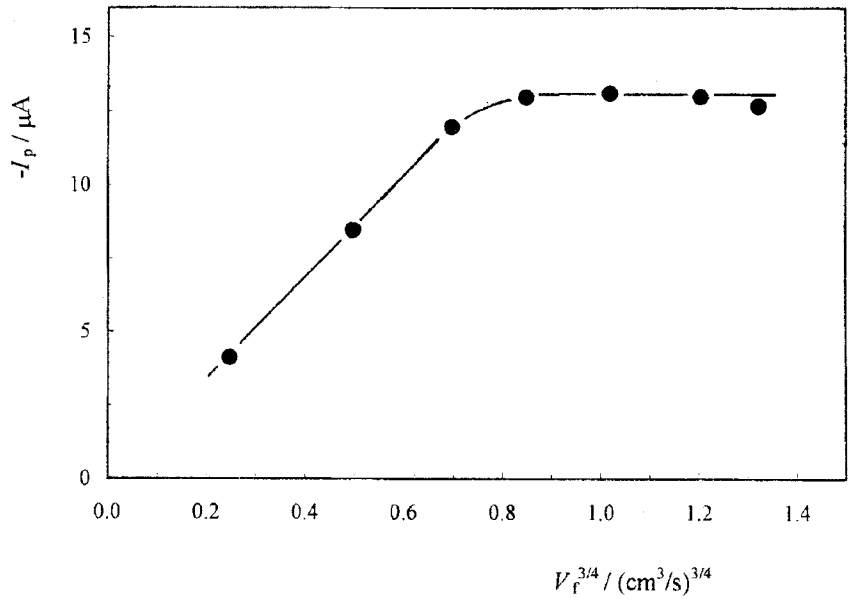

Fig. 2. Effect of flow rate on peak current, I_p, for SWAdSV of Co^{2+} (1.00×10^{-8} mol dm^{-3}); square wave frequency 100 Hz. Other conditions as in Figure 1.

However, in adsorptive stripping voltammetry flow effects in the determination step are minimal since the reagent is adsorbed on the mercury surface and the product of the reduction reaction dissolves in the mercury film. The asymmetry of the AdSV current peak has been observed experimentally by others and modeled theoretically for the irreversible square wave voltammetry of adsorbed reactants [14,15]. Peak half-widths are 32 mV for nickel and 49 mV for cobalt which, at first sight, suggests slower reduction kinetics for cobalt. Nevertheless, it should be recalled that there is a catalytic effect in this case, probably involving recycling between Co^{I} and Co^{II} [16], which could lead to larger values of peak width.

3.1. Solution Flow Rate

The effect of solution flow rate, V_f, is demonstrated in Figure 2 for cobalt. A linear variation of peak current, I_p, with $V_f^{3/4}$ as predicted from the limiting current equation for the wall-jet electrode [17], valid during adsorption accumulation, is found for flow rates up to around $0.035\,cm^3\,s^{-1}$ ($V_f^{3/4} = 0.081$) and which therefore represents maximum sensitivity. At higher flow rates the response does not increase with increasing flow rate. Previous work involving other techniques with wall-jet electrode cells of exactly the same geometry has shown no limitation of this kind at flow rates above $0.035\,cm^3\,s^{-1}$ [18], so that such behavior is not due to

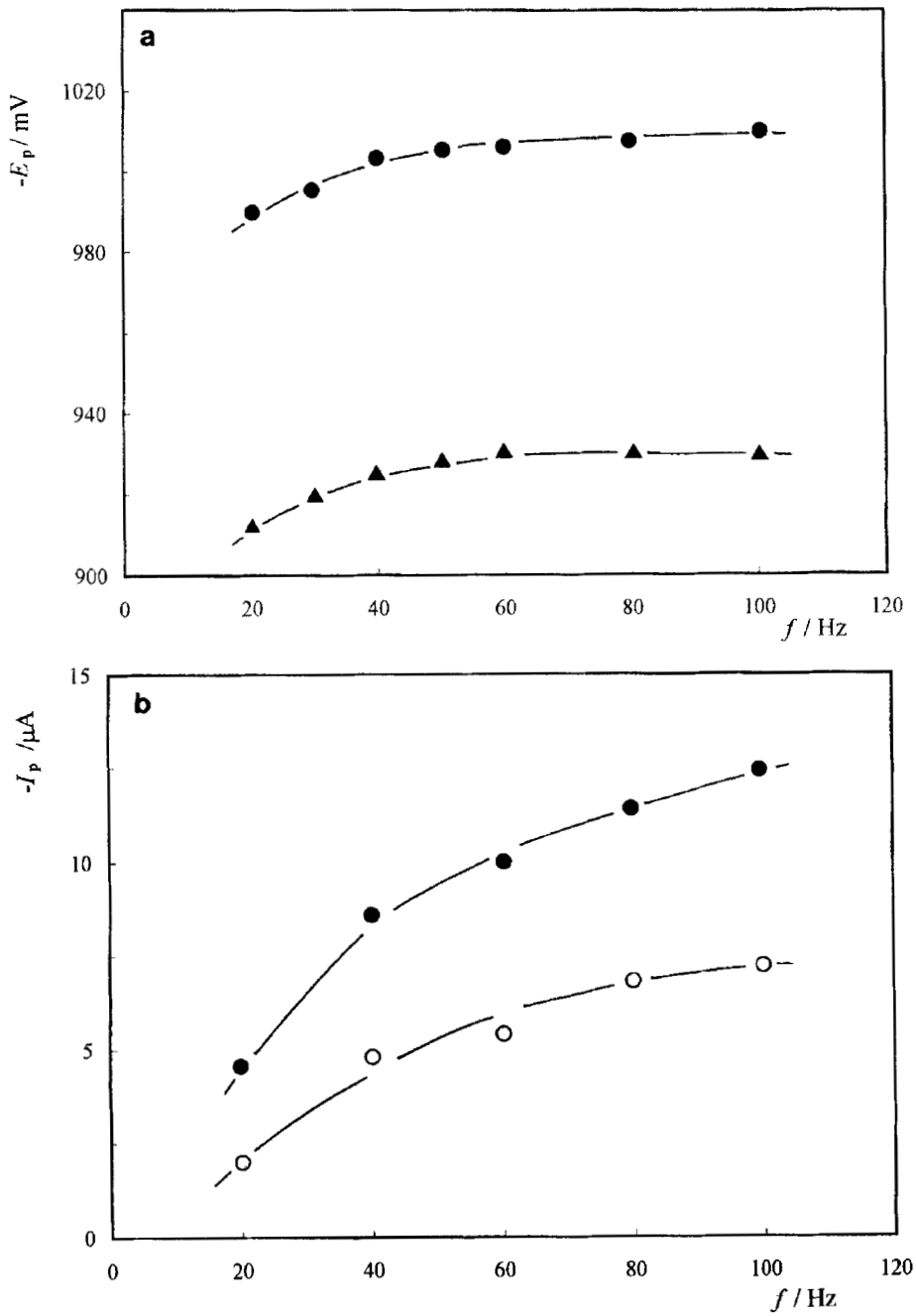

Fig. 3. a) Dependence of peak potential, E_p, on square wave frequency for SWAdSV of cobalt (●) and nickel (▲) ions. $[Ni^{2+}] = [Co^{2+}] = 6.0 \times 10^{-9}$ M. b) Effect of square wave frequency of SWAdSV peak current for Co. $[Co^{2+}]$: ○ 6.00×10^{-9} mol dm^{-3}, ● 1.00×10^{-8} mol dm^{-3}. Other conditions as Figure 1.

defective cell design. A possible explanation lies in the fact that the high convection reduces the diffusion layer thickness to such an extent that the necessary adsorption/desorption equilibrium is unable to occur under natural conditions during the accumulation step. A flow rate of 0.035 $cm^3 s^{-1}$ was chosen for all subsequent experiments.

3.2. Square Wave Parameters

In optimizing the conditions for the SWAdSV experiment, particular attention was paid to the influence of square wave parameters. Figure 3 shows the dependence on square wave frequency, f, of peak potential, E_p, and peak current, I_p. Examination of Figures 3a, b shows some similar variations. The negative variation of peak potential with increasing frequency becomes less for frequencies above 40 Hz as does the variation of peak current. The reasons can be traced to electrode kinetic effects during the negative-going square wave scan at the higher frequencies, also reflected in increasing values of the peak width at half-height. These results are identical for the ions separately and in mixtures. The approximate relationship

$$E_p = \text{constant} + (RT/\alpha nF)\ln(k^0/2f) \quad (1)$$

where k^0 is the standard rate constant and all other symbols have their usual meaning was suggested in [14]. However, although a plot of E_p vs. ln f only leads to reasonably good straight lines, the line of best fit permits the calculation of (αn) for the case of nickel (which does not follow a catalytic mechanism) and gives to a value of ca. 1.7 which is in reasonable agreement with that calculated from the approximate expression for half-width [14]

$$W_{1/2} = (63.5 \pm 0.5)/\alpha n \quad (2)$$

valid for sufficiently high square wave amplitudes. Such a value clearly suggests that the second electron transfer is rate-determining.

Concerning square wave amplitude, within the range tested up to 50 mV, the peak potential varies linearly with this parameter as does the peak current, the former becoming more positive by about 20 mV for each 10 mV increase in amplitude. As occurs for the variation with square wave frequency, separation between the nickel and cobalt peak potentials remains constant. Nevertheless, in order to avoid complications from effects of electrode kinetics, it is not prudent to employ very large square wave amplitudes. Thus, values of a square wave amplitude of 30 mV and a square wave frequency of 100 Hz were chosen in order to maximize sensitivity.

3.3. Adsorption Time

As in other adsorptive stripping voltammetric procedures, the increase of adsorption time leads to attainment of a maximum response, due to equilibrium saturation of the electrode surface for that analyte concentration in solution (Fig. 4). The accumulation time for which the response levels off is approximately the same as that obtained in the equivalent differential pulse experiment at the wall-jet electrode [10]. For this reason, the adsorption time chosen for calibration plots was 60 s which is still in the linear part of the plots, and therefore not subject to saturation effects.

3.4. Calibration Plots

Calibration plots were constructed for nickel and cobalt ions separately and in solutions containing the ions as a mixture. The enhancement factor for cobalt relative to nickel when analyzing metals separately and in the mixture is 1.8. This enhancement factor is due to catalytic effects and has been the object of investigation as indicated above [16]. Relevant parameters from the plots for the ions analyzed separately and in the mixture, under optimum conditions, are: nickel 0.63 μA/nM and 0.76 μA/nM, respectively, cobalt 1.27 μA/nM and 1.35 μA/nM, respectively. Intercepts are close to zero and regression

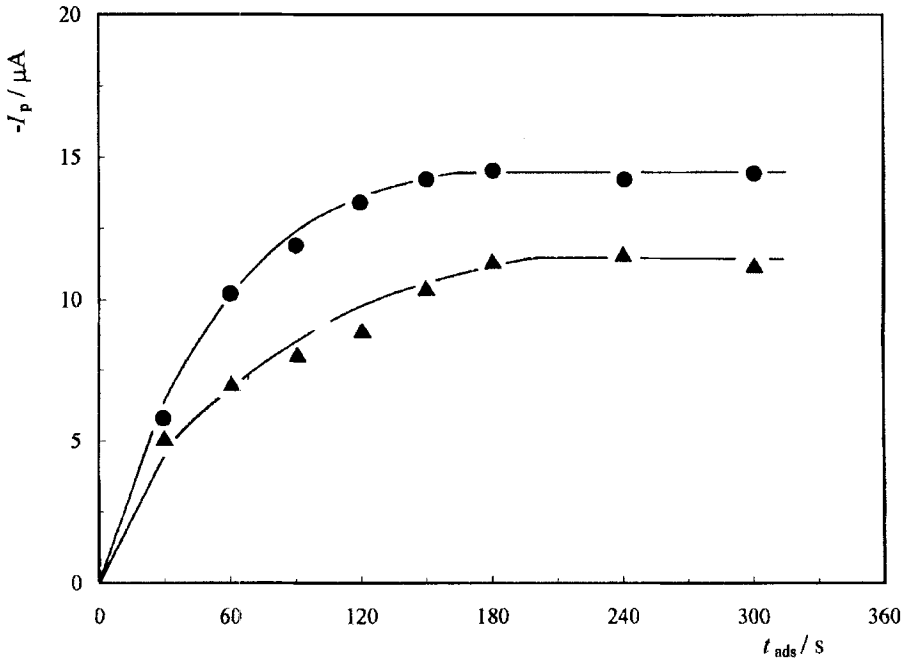

Fig. 4. Effect of adsorption time at f = 100 Hz on peak current for: Ni^{2+} (1.00×10^{-8} mol dm^{-3}) (▲) and Co^{2+} (8.00×10^{-9} mol dm^{-3}) (●). Other conditions as Figure 1.

coefficients are 99.5% or better in all cases. The higher values in the mixture are due to slight overlapping of the peaks. Practical detection limits are 1 nM, from signal-to-noise ratio a detection limit of 5×10^{-11} M being predicted in the absence of special precautions to eliminate noise. Above metal ion concentrations of 10^{-7} M saturation effects become problematic and the calibration plots are no longer linear. The slightly higher sensitivity in solutions containing both ions can be traced to the overlapping of the signals; however, reproducibility is not affected.

3.5. Comparison with Differential Pulse AdSV

The slopes of the calibration plots can be compared with those obtained in differential pulse AdSV of nickel and cobalt at the wall-jet electrode, which were 0.08 μA/nM and 0.17 μA/nM [10]. Square wave voltammetry results in a sensitivity enhancement by a factor of approximately ten. This is, however, not reflected in a lower practical detection limit, which is probably influenced mainly by slight irreproducibilities in the mercury film and to contamination effects. Other important benefits of square wave voltammetry are that deoxygenation of the analyte solution is not necessary and that the duration of the determination step is of the order of seconds rather than one to two minutes.

4. Conclusions

This work has shown the advantages of performing square wave adsorptive stripping voltammetry in continuous flow at a wall-jet mercury thin film electrode using the examples of nickel and cobalt. Advantages are to be gained relative to using differential pulse voltammetry in the determination step, through suppression of the necessity of deoxygenation of the sample solution and the faster determination step using square wave voltammetry. As a technique that can be used directly for on-line monitoring, it complements adsorptive stripping voltammetry by batch injection analysis [19], which permits the determination of small ($\leq 100\,\mu$L) discrete analyte samples.

5. References

[1] E.J. Underwood, *Trace Elements in Human and Animal Nutrition*, 4th ed., Academic Press, New York **1977**.
[2] K. Stulik, V. Pacakova, *Electroanalytical Measurements in Flowing Liquids*, Ellis Horwood, Chichester **1987**.
[3] C.M.A. Brett, M.M.P.M. Neto, *J. Chem. Soc. Faraday Trans. I* **1986**, *82*, 1071.
[4] J. Wang, *in Electroanalytical Chemistry*, Vol.16 (Ed: A.J. Bard), Dekker, New York **1989**, pp. 1–88.
[5] B. Pihlar, P. Valenta, H.W. Nurnberg, *Fresenius' Z. Anal. Chem.* **1981**, *307*, 337.
[6] A.M. Bond, D.L. Luscombe, *J. Electroanal. Chem.* **1986**, *214*, 21.
[7] J.R. Donat, K.W. Bruland, *Anal. Chem.* **1988**, *60*, 240.
[8] H. Zhang, R. Wallast, J.-C. Vire, G.J. Patriarche, *Analyst* **1989**, *114*, 1597.
[9] A. Economou, P.R. Fielden, *Analyst* **1993**, *118*, 47.
[10] C.M.A. Brett, A.M. Oliveira Brett, J.L.C. Pereira, *Electroanalysis* **1991**, *3*, 683.
[11] J.G. Osteryoung, J.J. O'Dea, in *Electroanalytical Chemistry*, Vol. 14 (Ed: A.J. Bard), Dekker, New York **1986**, pp. 209–308.
[12] M. Wojciechowski, J. Balcerzak, *Anal. Chem.* **1990**, *62*, 1325.
[13] C.M.A. Brett, A.M. Oliveira Brett, *J. Electroanal. Chem.* **1989**, *262*, 83.
[14] M. Lovric, S. Komorsky-Lovric, *J. Electroanal. Chem.* **1988**, *248*, 239.
[15] J.J. O'Dea, A. Ribes, J. Osteryoung, *J. Electroanal. Chem.* **1993**, *345*,287.
[16] A. Bobrowski, *Anal. Chem.* **1989**, *61*, 2178.
[17] C.M.A. Brett, A.M. Oliveira Brett, *Electrochemistry. Principles, Methods and Applications*, Oxford University Press, Oxford **1993**, p. 152.
[18] C.M.A. Brett, A.M. Oliveira Brett, A.C. Fisher, R.G. Compton, *J. Electroanal. Chem.* **1992**, *334*, 57.
[19] C.M.A. Brett, A.M. Oliveira Brett, L. Tugulea, *Electroanalysis*, **1996**, *7*, 639.